Received: 6 March 2018 | Accepted: 17 August 2018
DOI: 10.1111/jfb.13786

JOURNAL OF FISH BIOLOGY fsbi

REGULAR PAPER

A new species of *Diapoma* (Characiformes, Characidae, Stevardiinae) from the Rio Paraná basin, with an identification key to the species of the genus

James A. Vanegas-Ríos[1] | **María de las M. Azpelicueta**[1] | **Luiz R. Malabarba**[2]

[1]División Zoología de Vertebrados, Facultad de Ciencias Naturales y Museo, CONICET, UNLP, Paseo del Bosque S/N° B1900FWA, La Plata, Argentina

[2]Departamento de Zoologia, Laboratório de Ictiologia, Universidade Federal do Rio Grande do Sul (UFRGS), Instituto de Biociências, Porto Alegre, Brazil

Correspondence
James A. Vanegas-ríos, División Zoología de Vertebrados, Facultad de Ciencias Naturales y Museo, CONICET, UNLP, Paseo del Bosque S/N° B1900FWA, La Plata, Buenos Aires, Argentina.
Email: anyelovr@fcnym.unlp.edu.ar

Funding information
Fondo para la Investigación Científica y Tecnológica (AR), Grant/Award Number: BIP-PICT 2014-2357

Diapoma nandi is described from the Piray-Miní stream, a tributary of the Rio Paraná in Argentina. It is characterized among the Stevardiinae by having a terminal mouth, two unbranched and eight branched dorsal-fin rays, one unbranched and six branched pelvic-fin rays and the absence of a caudal-fin organ and is distinguished from all congeners by the following combination of characters: unmodified scales on the lower caudal-fin lobe, lack of enlarged opercle and subopercle, incomplete lateral line, hyaline adipose fin, anal-fin distal border straight or slightly convex in adult males, large tricuspid teeth on anterior region of the dentary, distal arrangements of the anal-fin bony hooks in adult males, middle caudal-fin rays lacking large round blotch and several morphometric variables associated with body shape. Additionally, we conducted a morphometric comparison focused on the congeners that co-occur in the Paraná basin.

KEYWORDS

endemic species, neotropical freshwater fish, Piray-Mini stream, sexual dimorphism, Stevardiinae

1 | INTRODUCTION

The freshwater genus *Diapoma* Cope 1894 has been traditionally placed within the tribe Diapomini sensu Weitzman and Menezes (1998), first proposed as monophyletic based on two synapomorphies associated with modified scales on the lower caudal-fin lobe of both females and males (Weitzman, 2003; Weitzman *et al*., 2005). Under this definition, *Diapoma* was grouped together with the genera *Acrobrycon* Eigenmann & Pearson 1924 and *Planaltina* Böhlke 1954 (Weitzman, 2003; Weitzman & Menezes, 1998; Weitzman *et al*., 2005). However, the monophyly of this tribe was recently refuted based on a more comprehensive phylogenetic analysis of Stevardiinae and, because of this, has been redefined to exclude *Acrobrycon* and to include nine other genera (Thomaz *et al*., 2015).

Based on DNA analyses, the species of *Cyanocharax* Malabarba & Weitzman 2003 and *Diapoma* sensu Menezes and Weitzman (2011) and *Hyphessobrycon guarani* Mahnert & Géry 1987 were resolved as a well-supported monophyletic group that was named *Diapoma* (Thomaz *et al*., 2015). Regardless of the lack of a morphological phylogenetic analysis, the authors claimed that the presence of one unbranched and six branched pelvic-fin rays might be considered a synapomorphy for the genus, differing from the other genera in Stevardiinae that have one unbranched and seven branched pelvic-fin rays (with some exceptions, such as *Lepidocharax* Ferreira, Menezes & Quagio-Grassiotto 2011 or *Planaltina*). This new generic definition enlarged the diversity of the genus from four to 13 valid species (Thomaz *et al*., 2015): *Diapoma alburnus* (Hensel 1870), *Diapoma alegretense* (Malabarba & Weitzman, 2003), *Diapoma dicropotamicus* (Malabarba & Weitzman, 2003), *D. guarani*, *Diapoma itaimbe* (Malabarba & Weitzman, 2003), *Diapoma lepiclastus* (Malabarba, Weitzman & Casciotta 2003), *Diapoma pyrrhopteryx* Menezes & Weitzman 2011, *Diapoma obi* (Casciotta, Almirón, Piálek & Říĉan 2012), *Diapoma speculiferum* Cope 1984, *Diapoma terofali* (Géry 1964), *Diapoma thauma* Menezes & Weitzman 2011, *Diapoma tipiaia* (Malabarba & Weitzman 2003) and *Diapoma uruguayense* (Messner 1962). More recently, as part of a total evidence analysis of

---

urn:lsid:zoobank.org:pub:7B6136B4-944E-4D67-829D-1F22A07123D0

Characidae, Mirande (2018) confirmed the definition of *Diapoma* sensu Thomaz *et al*. (2015). The *Diapoma* clade was supported by 18 molecular characters and three non-exclusive synapomorphies associated with the gill rakers, neurocranium and pelvic-fin rays (Mirande, 2018).

In the Rio de la Plata basin, eight species of *Diapoma* have been recorded (Almirón *et al*., 2016; Bertaco *et al*., 2016; Frota *et al*., 2016; Mahnert & Géry, 1987; Malabarba & Weitzman, 2003; Menezes & Weitzman, 2011; Protogino & Miquelarena, 2012; Zarucki *et al*., 2010): *D. alburnus*, *D. alegretense*, *D. guarani*, *D. lepiclastus*, *D. pyrrhopteryx*, *D. obi*, *D. terofali* and *D. uruguayense*. Only two of those species occur in the Paraná Basin, *D. guarani* and *D. obi* and are also present in Argentina (Mahnert & Géry 1987; Casciotta *et al*., 2012; Eschmeyer *et al*., 2018). The geographic records of those two species in Argentina are restricted to a few localities in Misiones Province: *Diapoma guarani* is known from the paratype specimens collected in the upper Rio Paraná at Montecarlo (Mahnert & Géry, 1987) and from a series of specimens from the Urugua-í stream (Parana Basin) that are revised here (MACN 7727), whereas *Diapoma obi* is present in tributaries of the Paranay-Guazú and Garuhapé drainages (Casciotta *et al*., 2012; Vanegas-Ríos, 2017). As part of a review of samples of *Diapoma* from the Paraguay–Paraná Basin, we found that some specimens from the Piray-Miní Drainage in Misiones correspond to a new species of the genus, which is described here. Additionally, an identification key to the species of *Diapoma* is provided.

2 | MATERIALS AND METHODS

The specimens studied are deposited in seven institutions: Fundación Miguel Lillo, San Miguel de Tucumán, Tucumán, Argentina (CI-FML), Laboratório de Biologia e Genética de Peixes, Departamento de Morfologia, Universidade Estadual Paulista “Júlio de Mesquita Filho,” Campus de Botucatu, São Paulo, Brazil (LBP), Laboratorio de Genética Evolutiva-Peces, Posadas, Argentina (LGEP), Museo Argentino de Ciencias Naturales “Bernardino Rivadavia”, Ciudad Autónoma de Buenos Aires, Argentina (MACN), Museu de Ciências e Tecnologia, Pontifícia Universidade Católica do Rio Grande do Sul, Porto Alegre, Rio Grande do Sul, Brazil (MCP), Museo de La Plata, La Plata, Buenos Aires, Argentina (MLP) and Muséum d'histoire naturelle, Genève, Switzerland (MHNG), with all abbreviations following Sabaj (2016). Counts of the pectoral, pelvic and dorsal-fin rays follow Böhlke (1958). Measurements and other counts were taken according to Fink and Weitzman (1974), with the addition of two measurements: anal-fin lobe length, following Menezes and Weitzman (1990) and the distance between dorsal and pectoral-fin origins, following Vanegas-Ríos *et al*. (2013). Measurements were taken point to point with digital callipers under a stereomicroscope and are expressed as percentages of standard length (L_S) or head length (L_H) for units of the head. Frequency of a particular meristic character is indicated in parentheses and holotype values are denoted by an asterisk. Numbers of radii were examined from scales from several regions of the body (areas: predorsal, lateral line with and without pore, pre-ventral and the base of the caudal fin). Specimens were cleared and stained (c&s) following Taylor and Dyke (1985). Total number of vertebrae were counted in c&s specimens. Those counts included the first pre-ural centrum plus first ural centrum (PU1 + U1) counted as one element and all four vertebrae of the Weberian apparatus. Specimens that were analysed from digitised photographs using tpsDig 2.26 (Rohlf, 2015) are indicated by an asterisk in 5. An identification key for the species of *Diapoma* was made based on our own observations and the data from Malabarba and Weitzman (2003) and Menezes and Weitzman (2011). *Hyphessobrycon procerus* Mahnert & Géry 1987 and *Hyphessobrycon wajat* Almirón & Casciotta 1999 were included in the diagnosis because of their morphological resemblance to the new species, especially regarding the shared presence of one unbranched and six branched pelvic-fin rays and two unbranched and eight branched dorsal-fin rays (Carvalho & Langeani, 2013). Furthermore, both species, particularly *H. wajat*, seem potentially to be *Diapoma* species (Mirande, 2018; J. Vanegas-Ríos, personal observation, 2018).

In order to compare the new species with the geographically closest congeners, the morphometric data were analysed through allometric Burnaby's correction method (Burnaby, 1966; Humphries *et al*., 1981; Rohlf & Bookstein, 1987), in which the morphometric variables were log-transformed and then projected onto a space orthogonal to the first principal component. The size-corrected morphometric variables of each studied species were analysed through a principal component analysis (PCA) and a discriminant canonical analysis (DCA). For the PCA analysis, the number of significant components was decided by two criteria: the broken-stick model (Frontier, 1976) and the scree plot method (Cattel, 1966). Comparative linear regressions were performed on the specimens studied (sexed by the absence–presence of bony hooks and in some cases by gonadal inspection) to detect characteristics associated with sexual dimorphism. For those analyses, normality was tested using a Shapiro–Wilk statistic (W) in each case ($\alpha < 0.05$) and data were log-transformed when needed. Statistical procedures were carried out in PAST 3.14 (Hammer *et al*., 2001) and Sigma Plot 12 (Systat Software, Inc.; www.systatsoftware.com).

3 | RESULTS

3.1 | *Diapoma nandi* sp. nov.

urn:lsid:zoobank.org:act:DD903205-B111-478C-8667-C0336DDAFFD3.

3.1.1 | Holotype

MLP 11309, male, 52.7 mm L_S, Argentina, Misiones Province, Eldorado, Rio Paraná basin, Piray-Miní stream, near bridge on National Route 12, *c*. 26° 20′ 59“S; 54° 37′ 05” W 128 m a.s.l. (above sea level), November 2000, M. Azpelicueta & E. Rodriguez (Figure 1).

3.1.2 | Paratypes

CI-FML 7282, two, 35.9–44·1 mm L_S; MACN 12472, two, 36.9–44.9 mm L_S; MLP 11311, 26, 30.1–46·8 mm L_S (two c&s, 37.6–43.6 mm L_S): Argentina, Misiones Province, Eldorado, Rio Paraná basin, Piray-Miní stream, near Balneario Eldorado, *c*. 26° 22′ 46“ S; 54° 34′ 20” W, 145 m a.s.l., October 1986, M. Azpelicueta, L. Braga & O. García. CI-FML 7283, six, 46.3–56.2 mm L_S (not completely measured); LGEP 791, two, 43.9–51.6 mm L_S; MLP 11310, four, 52.5–59.1 mm L_S, collected with holotype.

3.1.3 | Diagnosis

The presence of two unbranched and eight branched dorsal-fin rays and four (rarely five) teeth in the inner series of the premaxilla distinguishes *Diapoma nandi* from non-stevardiine characids (*v.* two unbranched and nine or more branched dorsal-fin rays and five or more teeth in the inner series of the premaxilla, except *H. procerus* and *H. wajat*) and from stevardiines of the tribe Eretmobryconini (*v.* two unbranched and nine or more branched dorsal-fin rays). *Diapoma nandi* is distinguished from *H. procerus* by body depth at dorsal-fin origin (32.4–38.8% L_S *v.* 26·1–30·1% L_S), the presence of a humeral mark (*v.* humeral mark absent) and head length (20.7–22.8% L_S *v.* 23.6–24.8% L_S) and from *H. wajat* by the different shape of the caudal-fin blotch, which is diffuse and much more concentrated on the peduncle (or partially on the interradialis muscles) than on the middle caudal-fin rays (*v.* well-defined dark rhomboidal blotch covering almost entire caudal-fin base) and the lack of an intense dark pigmentation at the basal half of the first two dorsal-fin rays (*v.* presence of such pigmentation).

The presence of six branched pelvic-fin rays (*v.* seven or more branched pelvic-fin rays) distinguishes *D. nandi* from other stevardiines, except some genera of Diapomini and Creagrutini (sensu Mirande, 2018), part of the Xenurobryconini and other species of *Diapoma*. *Diapoma nandi* is differentiated from the remaining diapomin genera by the combined presence of the following features: the anterior point of the snout aligned with the midpoint of the eye or on a point almost completely near to this (*v.* anterior point of snout notably aligned with upper or lower regions of eye, in some cases aligned with third infraorbital) and the teeth of the inner row of premaxillary dentition longer than those of the outer row (*v.* teeth of outer row of premaxillary dentition longer than those of inner row). The lack of modified scales on the caudal fin in adult males differentiates *D. nandi* from *Planaltina* and all members of the Xenurobryconini (*v.* caudal-fin organ in adult males) and from *D. pyrrhopteryx*, *D. speculiferum*, *D. thauma* and *D. terofali* (*v.* scales on the lower caudal-fin lobe forming a pocket-like structure in both sexes). *Diapoma nandi* is diagnosed from the other congeners by the following features: the absence of a posterior expansion of the opercle and subopercle (*v.* opercle and subopercle posteriorly expanded in *D. pyrrhopteryx* and *D. speculiferum*); the presence of an incomplete lateral line (*v.* complete lateral line in *D. alburnus*, *D. dicropotamicus* and *D. itaimbe*; rarely interrupted in *D. itaimbe*); a hyaline adipose fin (*v.* black adipose fin in *D. dicropotamicus* and *D. itaimbe*); the shape of the anal-fin distal margin in adult males, which is straight or slightly convex (*v.* distal border of this fin concave or strongly convex in *D. alegretense* and *D. uruguayense*); the number of cusps of the first three (often four) dentary teeth (three *v.* five to seven in *D. alegretense* and *D. uruguayense*).

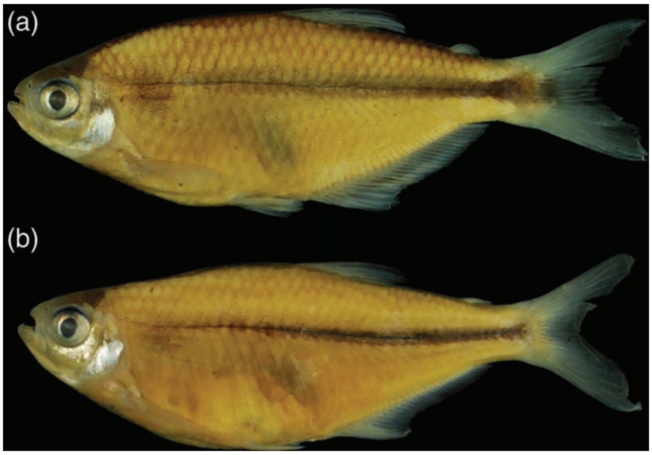

FIGURE 1 *Diapoma nandi* sp. nov., (a) MLP 11309, male, holotype, 52.7 mm standard length (L_S), Argentina, Misiones Province, Eldorado, Piray-Miní stream; (b) MLP 11310, female, paratype, 52.5 mm L_S, collected with holotype

Diapoma nandi is further diagnosed from *D. tipiaia* by the body depth at the dorsal-fin origin (32.4–38.8% L_S *v.* 28.5–31.3% L_S), greater horizontal eye length (37.1–45.4% L_H *v.* 31.5–37.0% L_H) and presence of a humeral mark (*v.* humeral mark absent); from *D. lepiclastus* by the larger distance between the snout and pelvic-fin origin (46.3–50.0% L_S *v.* 38.6–44.6% L_S) and larger distance between the snout and anal-fin origin (59.3–66.4% L_S *v.* 52.1–58.8% L_S); from *D. obi* by the larger distance between the dorsal and pectoral fin origins (39.3–42.5% L_S *v.* 43.1–48·0% L_S), lesser distance between the eye and dorsal-fin origin (43.5–45.7% L_S *v.* 47.1–49.8% L_S), number of cusps of the first three (usually four) dentary teeth in adults (three *v.* four to five), presence of a round humeral blotch (*v.* a vertically elongated humeral mark) and arrangement of the anal-fin bony hooks in adult males, which are more numerous and widely distributed on the distal portion of the rays (*v.* anal-fin bony hooks being more numerous and widely distributed on middle and basal portions of rays); and from *D. guarani* by the greater distance between the eye and the dorsal-fin origin (43.5–45.7% L_S *v.* 38.5–43.3% L_S), shorter head length (20.7–22.8% L_S *v.* 23.3–25.7% L_S), least interorbital width (34.1–39.9% L_H *v.* 27.7–33.8% L_H), total number of gill rakers on the first gill arch (18–21 *v.* 22–25) and position and shape of the caudal spot, which is much more concentrated on the caudal peduncle (or if partially on interradialis muscles not forming a conspicuous rounded pigmentation) than on the middle caudal-fin rays (*v.* large round blotch confined to the middle region of caudal fin).

3.1.4 | Description

Morphometric data are given in Table 1. Largest male 59.1 mm L_S, largest female 52.5 mm L_S. Body laterally compressed, maximum depth at vertical through area between pelvic and anal-fin origins (Figure 1). Dorsal head profile slightly convex (sometimes straight along midline of frontals); dorsal body profile convex from posterior end of supraoccipital area to dorsal-fin origin; straight and slanting ventrally from first dorsal-fin ray to caudal peduncle. Dorsal profile of caudal peduncle straight. Ventral body profile convex from tip of lower jaw to pelvic-fin origin, straight or slightly concave between pelvic and anal-fin origins, straight or slightly convex and slanting dorsally from this point to caudal peduncle. Ventral profile of caudal peduncle straight. Head with anterior region acute. Frontal fontanel present. Epiphyseal branch of supraorbital canal absent. Anterior nostril

TABLE 1 Morphometric data of *Diapoma nandi*. Identification of males based on presence of bony hooks on fins (range and mean S.D. of males include values of holotype)

		Males			Females and unsexed specimens		
	Holotype	Range	Mean ± S.D.	n	Range	Mean ± S.D.	n
Standard length (L_S, mm)	52.7	35.2–59.1	45.7 ± 6.8	20.0	31.0–52.5	36.5 ± 5.2	25
Percentages of L_S:							
Depth at dorsal-fin origin	35.7	34.5–38.8	36.3 ± 1.2	19.0	32.4–38.4	34.4 ± 1.5	20
Snout to dorsal-fin origin	56.0	53.6–57.8	55.0 ± 1.2	19.0	53.0–57.8	56.0 ± 1.3	20
Snout to pectoral-fin origin	25.8	25.0–26.8	25.7 ± 0.5	19.0	23.6–27.0	25.7 ± 0.8	19
Snout to pelvic-fin origin	47.2	46.4–50.0	47.8 ± 0.9	19.0	46.3–49.9	48.3 ± 1.1	20
Snout to anal-fin origin	62.2	59.8–64.9	62.1 ± 1.2	19.0	59.3–66.4	63.2 ± 1.9	19
Distance between dorsal- and pectoral-fin origins	42.5	39.3–42.5	41.1 ± 0.9	19.0	39.3–42.5	41.4 ± 0.9	20
Distance between dorsal- and adipose-fin origins	33.8	31.4–35.4	33.6 ± 1.0	19.0	30.1–35.1	32.2 ± 1.4	19
Dorsal fin to caudal-fin base	47.3	45.8–51.0	48.0 ± 1.4	19.0	44.4–49.8	46.7 ± 1.1	19
Eye to dorsal-fin origin	45.5	43.5–45.7	44.6 ± 0.7	19.0	43.5–45.3	44.6 ± 0.5	20
Distance between pectoral- and pelvic-fin insertions	22.9	21.1–25.0	22.7 ± 1.0	19.0	21.4–25.2	23.1 ± 1.0	19
Distance between pelvic- and anal-fin origins	15.4	14.4–17.2	15.8 ± 0.7	19.0	14.9–18.5	16.8 ± 1.0	19
Dorsal-fin length	22.1	21.7–24.4	23.3 ± 0.8	19.0	21.0–25.1	22.7 ± 0.9	19
Dorsal-fin base length	10.7	10.7–12.5	11.7 ± 0.4	19.0	9.1–12.2	10.7 ± 0.7	19
Pectoral-fin length	21.3	19.8–22.9	21.6 ± 0.9	19.0	19.3–22.7	21.4 ± 0.9	19
Pelvic-fin length	11.6	10.6–13.0	11.9 ± 0.6	19.0	11.8–13.2	12.4 ± 0.4	19
Anal-fin lobe length	15.9	14.0–16.7	15.5 ± 0.9	18.0	16.0–20.0	17.9 ± 1.1	19
Anal-fin base length	33.6	31.4–34.4	32.7 ± 0.8	19.0	28.5–32.1	30.4 ± 0.8	19
Caudal peduncle depth	12.2	10.4–12.2	11.6 ± 0.4	19.0	9.9–11.2	10.6 ± 0.4	19
Caudal peduncle length	12.3	10.5–13.3	12.0 ± 0.7	19.0	10.3–14.1	12.0 ± 1.0	19
Head length (L_H, mm)	21.3	21.1–22.8	21.9 ± 0.5	19.0	20.7–22.8	22.2 ± 0.6	20
Percentages of L_H							
Snout length	28.3	25.6–29.0	27.4 ± 1.1	17.0	23.8–28.7	26.6 ± 1.4	19
Horizontal eye length	38.8	37.1–41.8	40.3 ± 1.4	19.0	39.0–45.4	42.5 ± 1.9	19
Postorbital head length	41.9	38.8–41.9	40.3 ± 0.8	19.0	36.1–40.9	38.4 ± 1.1	19
Least interorbital width	35.2	35.2–39.9	36.9 ± 1.1	19.0	34.1–38.5	36.6 ± 1.3	20
Upper jaw length	40.6	38.0–44.0	41.4 ± 1.4	19.0	37.3–43.4	40.5 ± 1.8	18

n, Sample size.

rounded, separated by skin fold from posterior nostril; posterior nostril opening larger.

Mouth terminal, anterior tip of premaxilla horizontally aligned with upper half of eye. Premaxilla with two rows of teeth (Figure 2). Outer row with two (1), three* (16), four (19) or five (3) teeth; usually tricuspid, rarely conical. Inner row with four* (31) or five (8) teeth, symphyseal tooth tricuspid (often tetracuspid), remaining teeth tricuspid or tetracuspid. Maxilla with three (1), four (34) or five* (4) teeth (Figure 2); usually tricuspid or tetracuspid, rarely conical, bicuspid or pentacuspid. Posterior tip of maxilla surpassing vertical through anterior margin of eye, but not reaching anterior border of pupil. Dentary with nine (2), 10 (13), 11* (15), 12 (7) or 13 (3) teeth; three anteriormost teeth large, tricuspid; one median-sized tooth tricuspid (rarely tetracuspid) followed by five (2), six (13), seven* (15), eight (7) or nine (3) smaller tricuspid or conical posterior teeth (Figure 2).

Dorsal-fin rays ii (38), seven (1) or eight* (39). Nine proximal pterygiophores in dorsal fin (two c&s). Dorsal-fin origin at vertical slightly anterior to anal-fin origin, often reaching midpoint between anal and pelvic-fin origins. Adipose-fin origin at vertical crossing posteriormost two to four anal-fin rays. Anal-fin rays iv* (13) or v (27), 22(4), 23 (10), 24* (15), 25 (9) or 26 (2). Twenty-four to 26 proximal pterygiophores in anal fin (two c&s). Anal-fin origin at posterior half of body, always posterior to vertical through dorsal-fin origin. Pectoral-fin rays i (40),10 (19) or 11* (21). Pectoral-fin distal tip at vertical slightly behind pelvic-fin origin, sometimes reaching this origin. Pelvic-fin rays with i, six (40) in all specimens (most specimens with last ray simple but counted as branched). Pelvic-fin origin slightly anterior to midpoint of body. Caudal fin forked with 10/9 principal rays in all specimens.

Scales cycloid, with two to 12 radii along posterior region. Lateral line incomplete with eight* (4), nine (11), 10 (11), 11 (11) or 12 (3) anterior pored scales followed by 24 (1), 25 (2), 26 (2), 27 (9), 28 (15), 29 (7), 30* (3) or 31(1) non-pored scales; total number of lateral-line scales 35 (1), 36 (1), 37 (17), 38* (12), 39 (7), 40 (1) or 42(1). Terminal lateral-line tube absent on caudal-fin interradial membrane. Predorsal scales 12 (7), 13 (24) or 14 *(8), forming continuous row (one specimen with irregular row not counted). Five *(37) or six (3) scale rows between dorsal-fin origin and lateral line. Four scale rows between lateral line and anal-fin origin in all specimens. Three (1) or four* (39) scale rows between lateral line and pelvic-fin origin. Circumpeduncular scales 13 (2) or 14* (38). One row of scales forming sheath

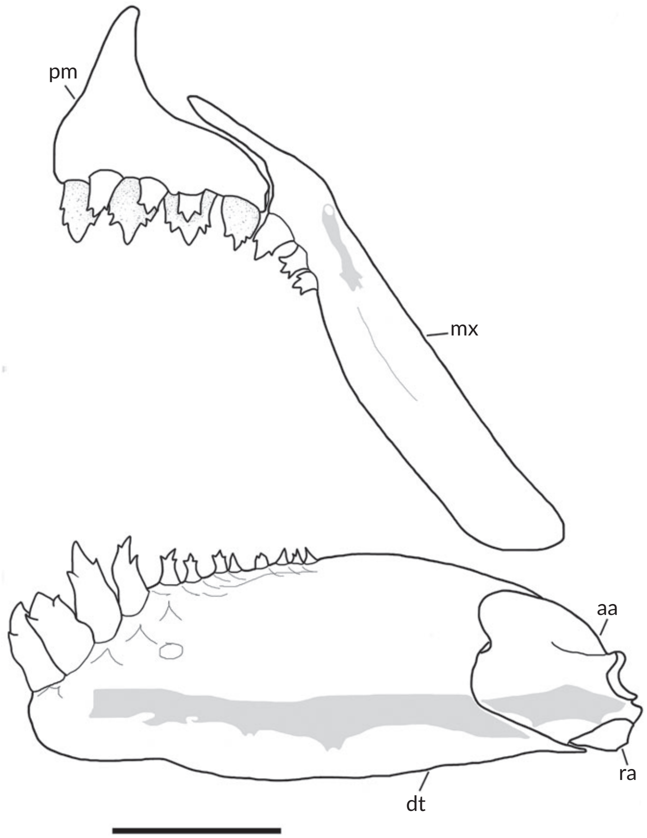

FIGURE 2 Jaws and dentition of *Diapoma nandi* sp. nov., MLP 11311, female, paratype, 37.9 mm standard length. aa: anguloarticular; dt: dentary; mx: maxilla; ra: retroarticular; pm: premaxilla. Left side. Scale bar: 1 mm

along anal-fin base (sometimes one additional row partially overlapping main row), with nine (2), 10 (1), 11 (4), 12* (9), 13 (5), 14 (8), or 15 (2) scales. Caudal-fin lobes covered by a set of four or five large unmodified scales, not extending beyond anterior one-third of each lobe. Total number of vertebrae 36 or 37 (two c&s), 16 precaudal and 20 or 21 caudal. Six (6), seven* (30) or eight (4) gill rakers on dorsal arm of first branchial arch; ventral arm with 12 (4), 13* (22) or 14 (14).

3.1.5 | Colour in alcohol

Ground colour pale yellowish in preserved males and females, slightly darker dorsally. Dark chromatophores on entire body, more diffuse on abdominal and ventral regions, but much more concentrated along mid-dorsal region, especially around adipose and dorsal fin. Round dark humeral blotch, diffuse in some specimens. Dark or silver midlateral stripe, extending from posterior region of humeral blotch to caudal peduncle. Large caudal-peduncle blotch, usually extending from middle region of peduncle to interradialis muscles, but in some specimens reaching half the length of middle caudal-fin rays. Few dark chromatophores forming stripes between myomeres on posterior ventral one-third of body. Dorsal fin mostly hyaline anteriorly but somewhat dusky posteriorly, with dark chromatophores much more concentrated on interradial membranes than on rays. Adipose fin mostly hyaline, with few scattered dark chromatophores.

Anal fin somewhat dusky throughout, with dark chromatophores much more concentrated on interradial membranes than on rays; distal border of fin darkly pigmented. Caudal fin mostly hyaline, with scattered dark chromatophores on rays and interradial membranes. Pectoral and pelvic fins mostly hyaline with dark chromatophores on interradial membranes and rays. Head darker dorsally; anterior region of isthmus and snout with somewhat darker pigmentation. Dark chromatophores extending around border of orbit. Opercle somewhat lighter, with scarce dark chromatophores. Infraorbitals pale yellowish (rarely somewhat silvery), with scattered dark chromatophores.

3.1.6 | Colour in life

Mid-dorsum with dark black stripe, more intensely marked between dorsal and adipose fins. Orbit bounded by dark chromatophores. Cheek pigmented with dark chromatophores. First four dorsal-fin rays whitish, posterior rays and interradial membranes, from ray 4 up to posteriormost ray, with dense reddish or orangish tonality. Adipose-fin base densely pigmented with dark chromatophores, less intense in females than in males. Anal-fin distal margin with reddish pigmentation, less intense in females than in males. Caudal peduncle spot variably developed among specimens, usually reaching tips of middle caudal-fin rays. Lateral stripe extending from upper margin of opercle to caudal peduncle, being wider on region of body located posterior to dorsal-fin origin. Chromatophores on lateral stipe larger than those on other portions of body. Humeral blotch consisting of grey chromatophores, densely pigmented in most specimens; secondary smaller light grey mark present.

3.1.7 | Sexual dimorphism

Males differ from females by the presence of bony hooks on the pelvic and anal-fin rays. All pelvic-fin rays of males bear short slender hooks that are oriented anterolaterally along middle region of rays. The pelvic-fin bony hooks are arranged in one row composed of several hooks that extends across the medial branch of most rays but the first and last rays. The anal fin of males has one to 18 variable-sized antrorse hooks distributed in two pairs per segment (rarely one pair) and are positioned mainly on the lateral or posterior surface of most anal-fin rays (ranging between the first branched ray up to 23rd ray). The anal-fin bony hooks are more numerous and larger on the anterior half of the fin and are confined to the distal portion of the posterior branch of each ray (Figure 3a).

Males usually have an intense dark pigmentation on the interradial membranes of the posteriormost four dorsal-fin rays (sometimes the chromatophores are also present on the rays); in life this pigmentation is reddish and orangish (anterior portion of fin is whitish). In females, the dorsal fin is less intensely pigmented, with scattered dark chromatophores on the interradial membranes. Most of the anal-fin interradial membranes are much more intensely pigmented with dark chromatophores in adult males than in adult females. The anal-fin distal margin is straight and more darkly pigmented in adult males (in life, this pigmentation is reddish), whereas it is concave and somewhat lighter in adult females. The gill gland was not observed in any specimens (the gill filaments were not found to be externally modified). Based on the morphometric comparisons (Table 1), three measurements showed differences between sexes in the comparative linear

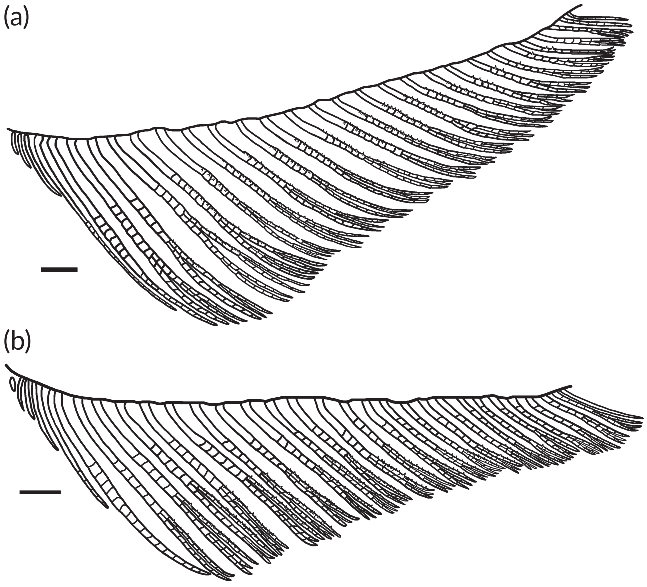

FIGURE 3 Anal fin showing the arrangement of bony hooks in adult males of (a) *Diapoma nandi* sp. nov., MLP 11311, male, paratype, 43.6 mm standard length (L_S); (b) *D. obi*, MACN 9557, male, paratype, 51.8 mm L_S. Left side. Scale bar: 1 mm

regressions performed (Figure 4 and Table 2): anal-fin lobe length, anal-fin base length and caudal peduncle depth.

3.1.8 | Distribution

Diapoma nandi is only known from its type locality, Piray-Miní stream (Figures 5 and 6).

3.1.9 | Etymology

The species name, *nandi*, is a word derived from the Guaraní language, which means inconsequential in allusion to the absence of remarkable external characteristics.

3.1.10 | Multivariate morphometric comparison

Comparing *D. nandi* with *D. guarani* and *D. obi* (its closest congeners in geographical terms), the plot of the first principal component (PC1: 28·5% of the total variance) *v.* the second principal component (PC2: 21.8% of the total variance) (Figure 7a) shows that individuals of *D. nandi* along PC1 were mainly separated from the individuals of *D. obi*, with *D. guarani* being intermediate between these. PC1 was loaded most heavily by the following measurements: negatively by the pelvic-fin length (−0.76) and upper jaw length (−0.21); and positively by the anal-fin lobe length (0.35), anal-fin base length (0.24) and dorsal-fin length (0.21). The positive loadings that most influenced

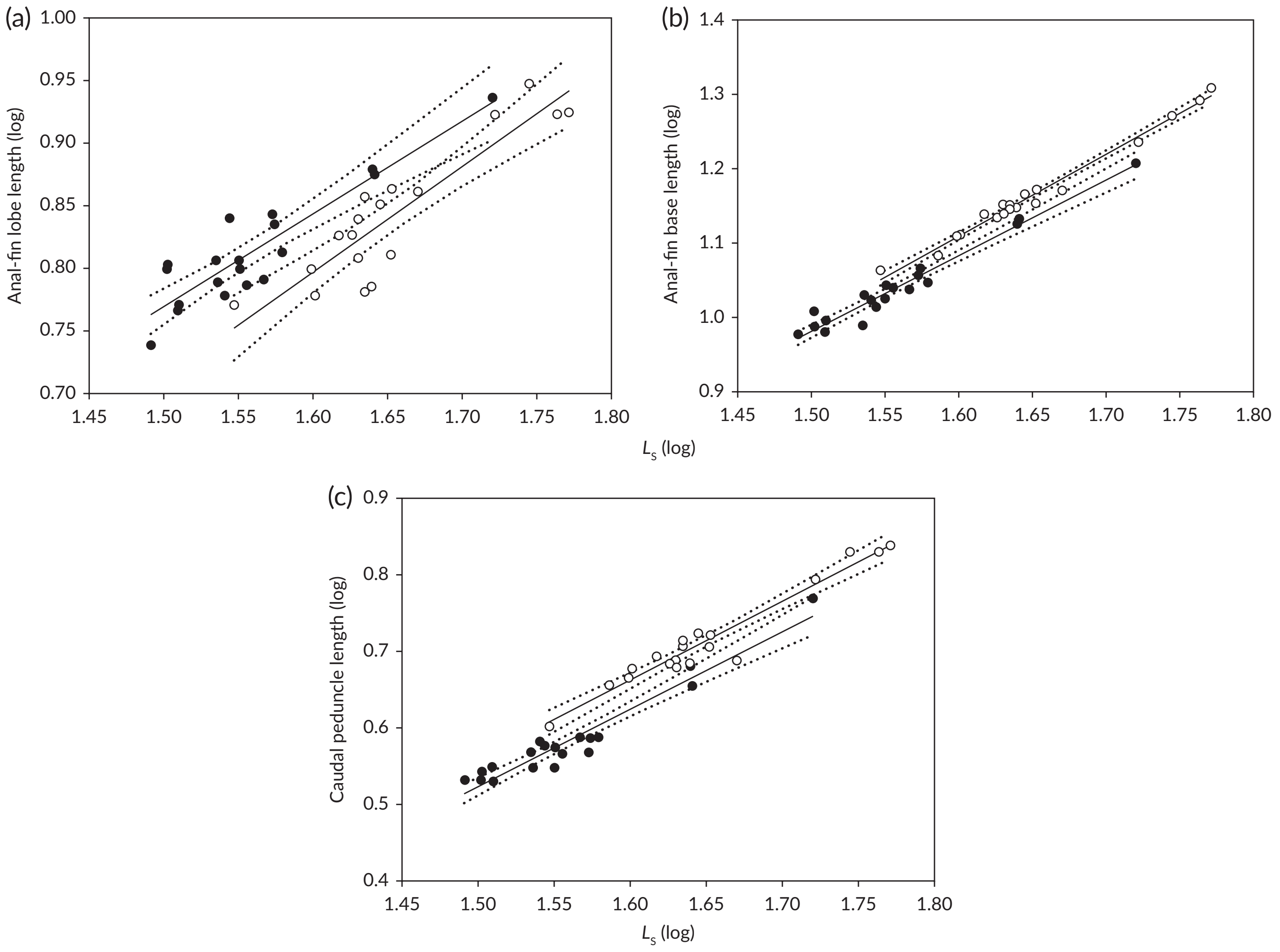

FIGURE 4 Comparative regression plots of females and males of *Diapoma nandi* sp. nov. standard length (L_S) and (a) anal-fin lobe length, (b) anal-fin base length, (c) caudal peduncle length. (Regression parameters are given in Table 2). (●) Female and juveniles, (○) Males and (┈┈) 95% Confidence line

TABLE 2 Results of comparative regressions performed between sexes of *Diapoma nandi*, using the morphometric variables as function of standard length that were observed partially sexually dimorphic

							β_0				β_1			
Regressions	**Sex**	***n***	***P***	***r***	***r2***	r^a		**S. E.**	***t***	***P***		**S. E.**	***t***	***P***
Anal–fin lobe length	Male	18	> 0.05	0.90	0.81	0.80	0.84	0.10	8.56	< 0.05	0.97	0.12	8.29	< 0.05
	Female	19	> 0.05	0.91	0.82	0.81	–0.34	0.13	–2.62	< 0.05	0.74	0.08	8.89	< 0.05
Anal–fin base length	Male	19	> 0.05	0.99	0.99	0.98	–0.65	0.05	–11.85	< 0.05	1.10	0.03	33.17	< 0.05
	Female	19	> 0.05	0.98	0.96	0.96	–0.54	0.08	–6.86	< 0.05	1.02	0.05	20.08	< 0.05
Caudal peduncle depth	Male	19	> 0.05	0.97	0.94	0.94	–0.99	0.10	–9.54	< 0.05	1.03	0.06	16.46	< 0.05
	Female	19	> 0.05	0.96	0.93	0.93	–1.00	0.11	–9.38	< 0.05	1.01	0.07	14.90	< 0.05

β_0: intercept; β_1: slope; *n*: Sample size; *r*: parametric correlation coefficient; r^2: determination coefficient; r^a: adjusted determination coefficient; S.E: standard error; *t*: Student's statistics.

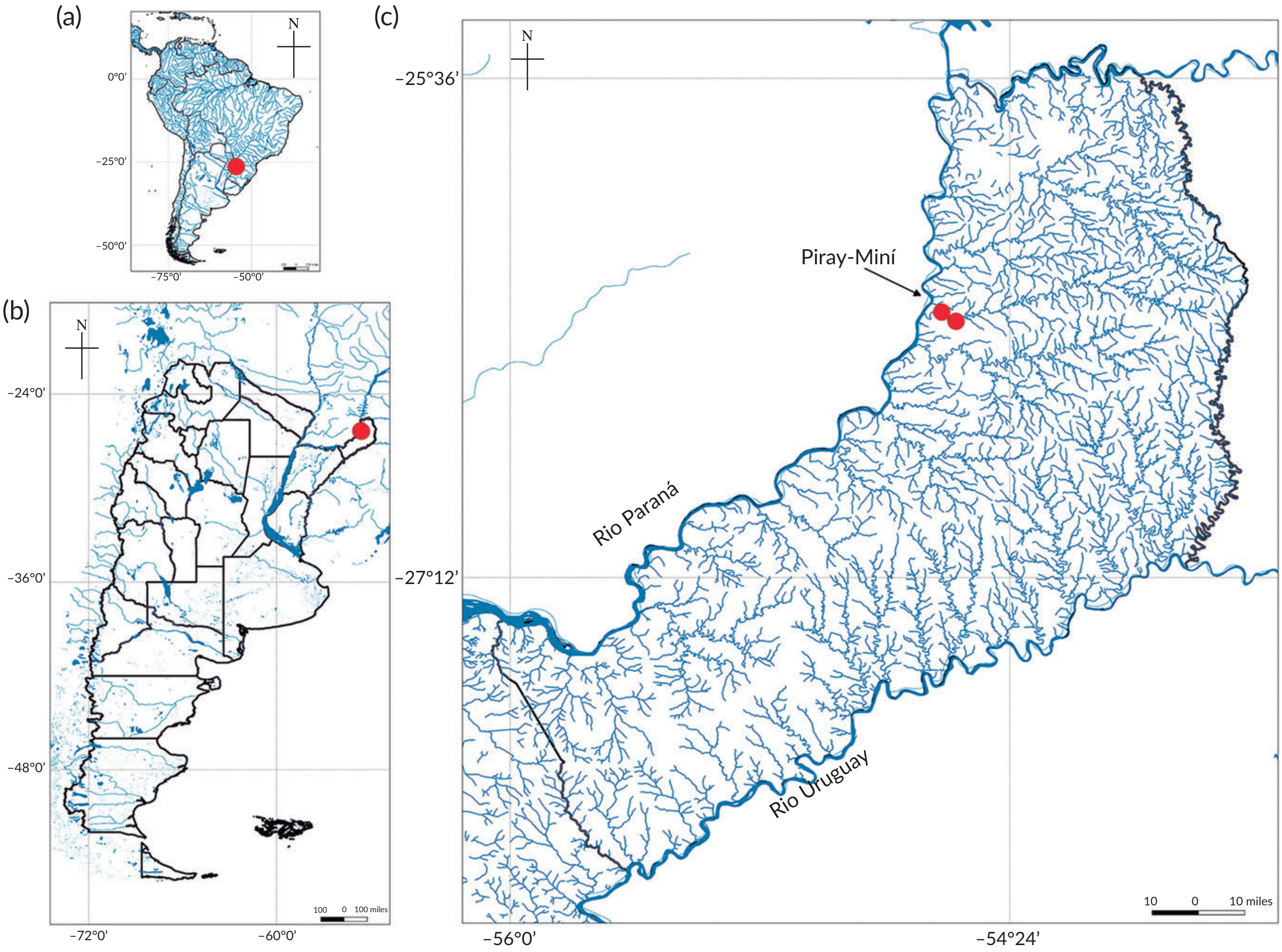

FIGURE 5 Geographical distribution of *Diapoma nandi* sp. nov. (●) in (a) South America, (b) Argentine and (c) the Rio Paraná basin in Misiones Province. Holotype locality corresponds to westernmost point in (c)

PC2 were the anal-fin lobe length (0.80) and pelvic-fin length (0.30), whereas the negative loading that most affected this component were the anal-fin base length (–0.23), upper jaw length (–0.22) and depth at dorsal-fin origin (–0.20). Although the scree-plot method and broken-stick model suggested the use of the first three components (62.0% of the total variance), the variability along PC3 (11.7% of the total variance) was not useful to separate the species and consequently the respective plot is not presented here. A size-free DCA partially discriminated *D. nandi* from *D. guarani* and completely discriminated *D. nandi* from *D. obi* along the first canonical axis (CA1: 98.2% of the total variance) (Figure 7b). The most important loading affecting CA1 was pelvic-fin length (0.01), while the second canonical axis (CA2) was most influenced by the anal-fin lobe length (0.03).

3.2 | Key to species of *Diapoma*

1a. Presence of modified scales on lower caudal-fin lobe, slightly more pronounced in adult males, forming a pocket-shaped structure ....2.

1b. Absence of modified scales on lower caudal-fin lobe, caudal scales at base never forming a pocket-shaped structure......................3.

FIGURE 6 Type locality of *Diapoma nandi* sp. nov. Piray-Miní stream, Paraná Basin, Misiones Province, Argentina. November, 2017

2a. Opercle and subopercle unmodified, not posteriorly prolonged..........4.

2b. Opercle and subopercle modified, posteriorly prolonged........5.

3a. Complete lateral line..........6.

3b. Incomplete lateral line..........7.

4a. 11–13 gill rakers on lower limb of first gill arch.........*D. thauma.*

4b. 15–18 gill rakers on lower limb of fist gill arch..........*D. terofali.*

5a. Snout length 21.3–24.5% L_H; maxillary teeth pentacuspid; live specimens with intense red pigmentation on some portions of all fins except pectoral fin (see Menezes & Weitzman, 2011: Figure 34; Almirón *et al*., 2016: Figure 2)..........*D. pyrrhopteryx.*

5b. Snout length 17.0–21.4% L_H; maxillary teeth tricuspid (rarely with more cusps); no red coloration on any fin in live specimens..........*D. speculiferum.*

6a. Anal fin unpigmented, without distinctive marks; adipose fin not pigmented in preserved mature males and females; snout to pelvic-fin origin 48.1–52.6% L_S..........*D. alburnus.*

6b. Anal fin pigmented, with distal tip of anterior lobe unpigmented; adipose fin dark in preserved mature males and females; snout to pelvic-fin origin 40.4–46.6% L_S ....8.

7a. In adult males, anal-fin distal margin strongly convex ....9.

7b. In adult males, anal-fin distal margin straight or slightly convex ....10.

8a. Number of scale rows between dorsal and pelvic-fin origins 11–13.......... *D. itaimbe.*

8b. Number of scale rows between dorsal and pelvic-fin origins 9–11..........*D. dicropotamicus.*

9a. Anal-fin sheath consisting of 20–28 aligned scales, covering three-quarters or entire length of anal-fin base (usually reaching 22nd branched ray); 29–35 branched anal-fin rays (usually 29–33) ....*D. uruguayense.*

9b. Anal-fin sheath consisting of 23–30 aligned scales reaching no more than half length of anal-fin base (usually extending to 12th or 18th branched ray); 23–30 branched anal-fin rays (usually 25–27)..........*D. alegretense.*

10a. Snout to pelvic-fin origin 38.6–45.3% L_S..........11.

10b. Snout to pelvic-fin origin 46.3–52.7% L_S..........12.

11a. Horizontal eye length 31.5–37.0% L_H; anal-fin base length 27.9–31.3% L_S; diffuse or absent humeral mark ....*D. tipiaia.*

11b. Horizontal eye length 39.1–45.4% L_H; anal-fin base length 32.8–40.0% L_S; well-defined dark humeral mark ....*D. lepiclastus.*

12a. Middle and distal portions of interradial membranes of posterior branched dorsal-fin rays hyaline or, when faintly dusky, being similarly pigmented in both sexes; distance between dorsal and pectoral-fin origins 43.1–48.0% L_S; eye to dorsal-fin origin 47.1–49.8% L_S; first three (often four) dentary teeth tetra or pentacuspid in adults.......... *D. obi.*

12b. Middle and distal portions of interradial membranes of posterior branched dorsal-fin rays dusky, intensely darker in adult males than in females or juveniles; distance between dorsal and pectoral-fin origins 38.0–42.5% L_S; eye to dorsal-fin origin 38.5–46.4% L_S; first three (usually four) dentary teeth tricuspid in adults..........13.

13a. Presence of large dark round blotch on middle region of caudal fin, more noticeable in males; urogenital region darkly pigmented in females; eye to dorsal-fin origin 38.5–43.3% L_S; head length 23.3–25.7% L_S; least interorbital width 27.7–33.8% L_H; 5–10 maxillary teeth (mode = 5); 20–23 branched anal-fin rays (mode = 21); 22–25 gill rakers on first gill arch (mode = 23, 8–9 + 14–17); known body size 17.9–30.5 mm L_S ....*D. guarani.*

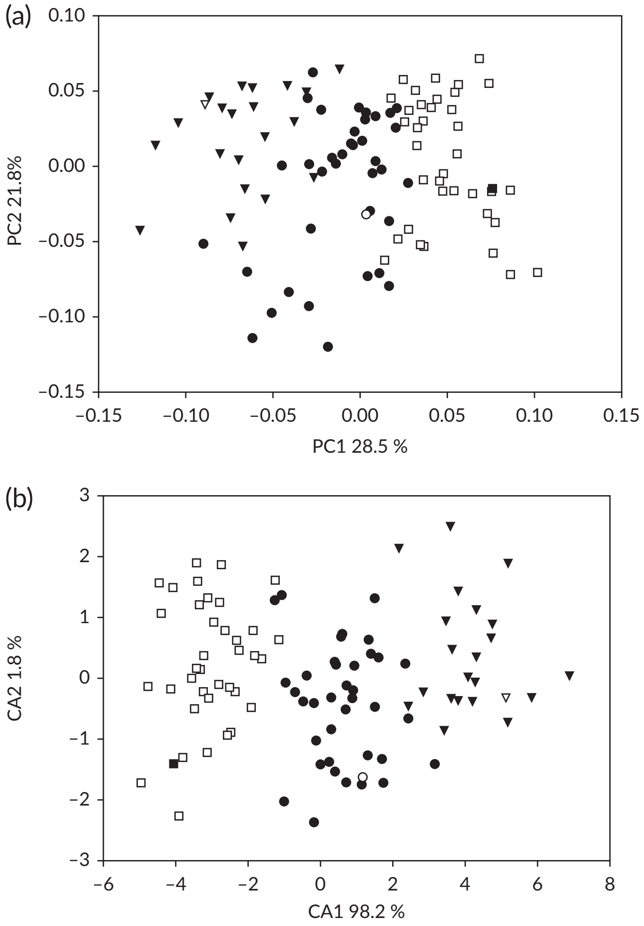

FIGURE 7 Multivariate comparison among *Diapoma nandi* sp. nov., *D. guarani*, and *D. obi* based on the morphometric data. (a) Size-corrected principal component analysis; (b) size-corrected discriminant canonical analysis. CA: canonical axis; PC: principal component. (●) *D. guarani*, (□) *D. nandi*, (▼) *D. obi*, (○) Holotype of *D. guarani*, (■) Holotype of *D. nandi* and (▽) Holotype of *D. obi*

13b. Absence of large dark blotch on middle region of caudal fin, with caudal spot much more concentrated on peduncle (or partially on interradialis muscles) than on middle caudal-fin rays (rarely faintly scattered dark chromatophores reaching midpoint of ray); urogenital region unpigmented in females; eye to dorsal-fin origin 43.5–45.7% L_S; head length 20.7–22.8% L_S; least interorbital width 34.1–39.9% L_H; 3–5 maxillary teeth (mode = 4); 22–26 branched anal-fin rays (mode = 24); 18–21 gill rakers on first gill arch (mode = 20, 6–8 + 12–14); known body size 31.0–59.1 mm L_S....................*D. nandi.*

4 | DISCUSSION

Diapoma nandi shares the following morphological characters that have been proposed as synapomorphies of Stevardiinae by Mirande (2010), Mirande *et al.* (2013), Vanegas-Ríos (2017) and Mirande (2018): absence of the epiphyseal branch of the supraorbital canal; presence of eight or fewer branched dorsal-fin rays; presence of nine dorsal-fin pterygiophores; dorsal margin of the lateral ethmoid anteriorly oriented in dorsal view; ventral margin of third infraorbital reaching the horizontal arm of the preopercle; presence of four or fewer (rarely five) teeth on the inner premaxillary row; dorsal margin of the third postcleithrum reaching or surpassing the midpoint of the second-postcleithrum; short frontal fontanel, reaching up to two-thirds the length of the parietal fontanel; ventral margin of the anguloarticular crosses perpendicularly to the dentary laterosensory canal; ectopterygoid is expanded lateral to the blade of the lateral ethmoid.

With regard to the stevardiine tribes proposed by Thomaz *et al.* (2015) that have been morphologically diagnosed by Mirande (2018: Diapomini, Eretmobryconini, Hemibryconini and Stevardiini) with minor changes in their composition, it is possible to conclude that *D. nandi* may be included in Diapomini because it shares a relatively large foramen or concavity on the lamella ventral to the supraoccipital spine (the only morphological synapomorphy supporting this tribe). Additionally, *D. nandi* does not share the distinctive characteristics or synapomorphies of the Eretmobryconini (Mirande, 2018; Thomaz *et al.*, 2015: except character 427), Gladulocaudini (Menezes & Weitzman, 2009), Hemibryconini (Mirande, 2018), Stevardiini (Mirande 2018; Vanegas-Ríos, 2017) and Xenurobryconini (Mirande, 2018; Vanegas-Ríos, 2017; Weitzman & Fink, 1985: except character 123). Despite the fact that the tribe Creagrutini was not morphologically diagnosed by Mirande (2018), the distinctive characteristics of most of its members, especially the *Carlastyanax* Géry 1972 + *Creagrutus* Günther 1864 clade, are not shared by *D. nandi* (Mirande *et al.*, 2013; Vanegas-Ríos, 2017).

Indeed, the morphology of the body, fins, jaws and dentition of *D. nandi* suggests that it may be a member of *Diapoma*, but what is most convincing is the fact that all synapomorphies proposed by Mirande (2018) for the genus are present in the species (neurocranial opening that communicates with the laterosensory canal of the sixth infraorbital located between the frontal and pterotic, 11 or more gill rakers on the first hypobranchial and ceratobranchial and six or less branched pelvic-fin rays). In any case, the phylogenetic placement of *D. nandi* should be tested using the matrices of Thomaz *et al.* (2015) and Mirande (2018) when tissues for DNA extraction and analysis become available.

It is worth mentioning that all species of *Diapoma* can be distinguished from the remaining members of the Diapomini sensu Thomaz *et al.* (2015) or Mirande (2018) and especially from those genera with similar number of branched pelvic-fin rays (*e.g. Planaltina* or *Lepidocharax* placed in Creagrutini sensu Mirande, 2018), by three additional morphological characters: the snout is aligned with the midpoint of the eye or with a point very near to this (*v.* snout clearly aligned with lower region of eye, in some cases aligned with third infraorbital) allows the distinction of *Diapoma* from *Attonitus* Vari & Ortega 2000, *Bryconacidnus* Myers 1929, *Ceratobranchia* Eigenmann 1914, *Piabarchus* Myers 1928 (except *P. torrenticola* Mahnert & Géry, 1988), *Piabina* Reinhardt 1867 and *Rhinobrycon* Myers 1944. *Diapoma* differs from *P. torrenticola* by the number of branched pelvic-fin rays (six *v.* seven, see Mahnert & Géry, 1988). Additionally, the characteristic position of the snout in species of *Diapoma* is different from that present in the *Lepidocharax* species, which have the anterior point of the snout aligned with the upper region of the eye. In *Diapoma*, the inner row of premaxillary teeth are longer than those of the outer row, whereas in *Attonitus*, *Bryconacidnus*, *Ceratobranchia*, *Bryconamericus lethostigmus* (Gomes 1947) (when it presents two rows of premaxillary teeth) and *Rhinobrycon* the outer row of premaxillary teeth are almost as long or longer than those of the inner row (additional comments on this type of dentition in Chernoff and Machado-Allison (1990), Vari and Ortega (2000) and Netto-Ferreira *et al*. (2014). Species of *Diapoma* have two different patterns of caudal-fin squamation: a set of two to five unmodified and relatively large scales covering the anterior one-third of each lobe and a set of multiple modified scales forming a pouch-like structure on the lower lobe (see Menezes & Weitzman, 2011). Both types of terminal caudal-fin squamation differ from those present in related genera such as *Planaltina* or *Lepidocharax*, especially in adult males (see further comparisons on the squamation of these genera in Menezes *et al*., 2003; Ferreira *et al*., 2011; Menezes & Weitzman, 2011; Deprá *et al*., 2018) and from the scaled caudal fins found in species of *Knodus* Eigenmann 1911 sensu Thomaz *et al*. (2015) or Mirande (2018).

Two characid species that occur in the Rio de la Plata basin, *H. wajat* and *H. procerus*, which resemble *D. nandi*, have been considered potential members of the Stevardiinae by having two unbranched and eight branched dorsal-fin rays and four (sometimes five) teeth in the inner series of the premaxilla (Carvalho & Langeani, 2013). Nevertheless, *D. nandi* is readily distinguishable from those species by the features mentioned above in the diagnosis. In a combined phylogenetic analysis of Characidae, Mirande (2018) recovered *H. wajat* in the Stevardiinae clade, supporting the hypothesis of Carvalho and Langeani (2013). Additionally, this species was obtained in the *Diapoma* clade (Mirande, 2018), based only on morphological data. It seems that the phylogenetic placements of *H. wajat* and *H. procerus* need to be revised using morphological and molecular data before changing their generic position (under ongoing study by J.A.V.R.).

When the overall morphological appearance of the body and size of *D. nandi* is compared with the remaining members of *Diapoma*, it is possible to notice that *D. nandi* is much more similar to those species that were initially placed in *Cyanocharax* sensu Malabarba and Weitzman (2003) than to those species that were initially placed in *Diapoma* (Menezes & Weitzman, 2011). In particular, comparing with the first species group that occurs in the Rio Paraná basin, the body shape of *D. nandi* is more similar to *D. guarani* than to *D. obi* (Figure 7). Additionally, as was mentioned in the diagnosis, *D. nandi* is easily distinguished from *D. guarani* and *D. obi* by a combination of other morphological characteristics, such as the number of gill rakers, the position and shape of the humeral and caudal marks, the number of cusps of the first three dentary teeth and the arrangement of the anal-fin bony hooks (Figure 3).

The circumscription of *D. nandi* in *Diapoma* is based on the morphological arguments associated with our current knowledge of the systematics of Stevardiinae, but this decision should be corroborated by a further molecular comparison among the species of the genus. Future studies on systematics of *Diapoma* need to be focused on testing its phylogenetic relationships using combined data sets.

5 | COMPARATIVE MATERIAL EXAMINED

Ceratobranchia obtusirostris Eigenmann 1914, MHNG 2183.050, one c&s, 29.0 mm L_S, Peru, Loreto, Rio Ucayali, Amazonia Peruana, Rio Huacamayo near Aguaytia. *Diapoma alburnus*, Brazil, Rio Grande do Sul, Porto Alegre, Praia das Pombas: CI-FML 3906, 2, 37.5–46.4 mm L_S; MCP 7054, 10, 30·8–57.3 mm L_S. *Diapoma alegretense*, MCP 25974, holotype, 37.5 mm L_S, Brazil, Rio Grande do Sul, Porto Alegre, creek on road Santa do Livramento-Alegrete, Alegrete. *Diapoma dicropotamicus*, MZUSP 82262, male, 42.5 mm L_S, Brazil, Rio Grande do Sul, Lageado, Lageado, Rio Forqueta, Marquês de Souza. *Diapoma guarani*, MACN 7727, 30, 18.9–23.4 mm L_S, Argentina, Misiones, Paraná basin, Urugua-í stream. MHNG 2366.99, holotype*, 31.7 mm L_S, Paraguay, Alto Paraná, Rio Paraná at Puerto Bertoni. MHNG 2366.100, five c&s (not measured), collected with holotype. MHNG 2370.013, seven (one c&s, 28.2 mm L_S), 22.5–28.2 mm L_S, Paraguay, Alto Paraná, Rio Paraná at Puerto Iguazú. *Diapoma itaimbe*, MCP 14290, 10, 39.4–44.6 mm L_S, Brazil, Rio Três Forquilhas, 29° 25′ 00“S, 50° 10′ 00” W. *Diapoma lepiclastus*, Argentina, Misiones, Uruguay basin, Fortaleza stream, 26° 45.5′ S, 54° 10′ W: MACN 9682, 47, 29·3–42·0 mm L_S, MLP 10451, five paratypes, 35·1–43.9 mm. *Diapoma obi*, CI-FML 3892, three c&s, 31.2–57.3 mm L_S; MLP 11312, three, 29.5–35.6 mm L_S: Argentina, Misiones, Aristóbulo del Valle, Moreno stream. MACN 9560, 52.6 mm L_S, Argentina, Misiones, Rio Paraná basin, tributary of the Paranay–Guazú stream, 26° 52′ 28.9″ S, 54° 42′ 22.8″ W. MACN 9557, nine, 37.9–51.8 mm L_S (1 c&s 51.8 mm L_S), same data as holotype. MACN 9558, 3, 37.6–44.7 mm L_S, tributary of the Paranay-Guazú stream, road 11 between Aristóbulo del Valle and El Alcazar, 26°.48′ 27“S; 54 ° 45′ 38” W. MACN 9559, three, 46.6–53.1 mm L_S, tributary of the Paranay-Guazú stream, road 11 between Aristóbulo del Valle and El Alcazar, 26° 48′ 27” S; 54° 45′ 38” W. MLP 10472, two, 52·2–57·4 mm L_S, tributary of the Paranay-Guazú stream in trail from road 14 to Montecarlo town, 26° 49′ 04“S; 54° 26′ 59” W. MLP 10897, one c&s, 58.7 mm L_S, tributary of the Paranay-Guazú stream, road 11 between Aristóbulo del Valle and El Alcazar, 26° 48′ 27” S; 54° 45′ 38” W. *Diapoma pyrrhopteryx*, MLP 10915, four, 51.9–53.1 mm L_S (one c&s, 49·5 mm L_S), Argentina, Misiones, Uruguay River basin, Toro stream, 26° 36′ 33“S; 53° 44′ 14” W. *Diapoma speculiferum*, MCP 7979, four, 31.3–43.3 mm L_S, Brazil, Rio Grande do Sul, Açude dos Garcia, Br-116 km, Barra do Ribeiro. *Diapoma terofali*, CI-FML 6101, one c&s, 35.7 mm L_S, Argentina, Entre Ríos, Concepción del Uruguay, El Sauce stream. *Diapoma tipiaia*, MCP 22766, 10 paratypes, 19.0–35.0 mm, Brazil, Rio Grande do Sul, Laguna dos Patos drainage, Tapiáia stream, about 13 km North of Júlio de Castilhos, on road to Cruz Alta, 29° 06′ 49“S; 53° 39′ 04” W. *Diapoma uruguayensis*, MACN 9681, 31.6–35.6 mm L_S, Argentina, Misiones, Uruguay basin, Itacaruaré stream 27° 52′ 34“S; 55° 16′ 35” W. See Additional examined of all *Diapoma* species but *Diapoma pyrrhopteryx*, *D. speculiferum*, *D. terofali* and *D. thauma* in Malabarba and Weitzman (2003). *Hyphessobrycon procerus*, MHNG 2385.069, five paratypes, 22.2–29.3 mm L_S, Paraguay, Caaguazu, á Ltr. Juan Frutos. *Hyphessobrycon wajat*, MLP 9321, holotype, 26.8 mm L_S, Argentina, Corrientes Province, Laguna Brava, 27° 33′ S; 58° 44′ W. *Lepidocharax burnsi* Ferreira, Menezes & Quagio-Grassiotto 2011, LBP 8990, two c&s, 28.6–27.3 mm L_S, Brazil, MG, Fortuna de Minas, Riacho without name 19° 37′ 34.1“ S; 44° 29′ 20.0” W. *Planaltina glandipedis* Menezes, Weitzman & Burns 2003, LBP 14618, two c&s, 27.5–29.1 mm L_S, LBP 14618, Brazil, SP, Botucatu, Rio Araquá 22° 44′ 50.2“S; 48° 28′ 30.5” W. *Piabarchus analis* (Eigenmann 1914), MHNG 2103.064, one, 31.3 mm L_S, Paraguay, Concepción, Estancia Sud d' Estrellas, Río Apa.

ACKNOWLEDGEMENTS

We are grateful to the following individuals and institutions for their assistance and support: G. Aguilera and J. Mirande (CI-FML); O. García (EBY-UNaM); M. Benitez (LGEP); I. García (ILPLA); G. Chiaramonte and R. Ferriz (MACN); S. Fisch-Muller and R. Covain (MHNG); and J. Casciotta, A. Almirón and D. Nadalin (MLP). We thank V. Mahnert for taking some data from the types of *D. guarani*. This research greatly benefited from a postdoctoral scholarship granted by CONICET to the senior author. Additional financial support was provided by FONCyT (BIP-PICT 2014–2,357, A. Cione and M. Azpelicueta) and CNPq (L. Malabarba).

ORCID

James A. Vanegas-Ríos https://orcid.org/0000-0001-9356-7687

REFERENCES

Almirón, A., Casciotta, J., Říčanová, S., Dragová, K., Piálek, L., & Říčan, R. (2016). First record of *Diapoma pyrrhopteryx* Menezes & Weitzman, 2011 (Characiformes: Characidae) from freshwaters of Argentina. *Ichthyological Contributions of PecesCriollos*, *40*, 1–3.

Bertaco, V. A., Ferrer, J., Carvalho, F. R., & Malabarba, L. R. (2016). Inventory of the freshwater fishes from a densely collected area in South America-a case study of the current knowledge of Neotropical fish diversity. *Zootaxa*, *4138*, 401–440. https://doi.org/10.11646/zootaxa.4138.3.1

Böhlke, J. (1958). Studies on fishes of the family Characidae.: No. 14. A report on several extensive recent collections from Ecuador. *Proceedings of the Academy of Natural Sciences of Philadelphia*, *110*, 1–121. https://doi.org/10.2307/4064529

Burnaby, T. P. (1966). Growth-invariant discriminant functions and generalized distances. *Biometrics*, *22*, 96–110. https://doi.org/10.2307/2528217

Carvalho, F. R., & Langeani, F. (2013). *Hyphessobrycon uaiso*: New characid fish from the rio Grande, upper rio Paraná basin, Minas Gerais State (Ostariophysi: Characidae), with a brief comment about some types of *Hyphessobrycon*. *Neotropical Ichthyology*, *11*, 525–536. https://doi.org/10.1590/S1679-62252013000300006

Casciotta, J., Almirón, A., Piálek, L., & Říčan, O. (2012). *Cyanocharax obi*, a new species (Characiformes: Characidae) and the first record of the genus from tributaries of the río Paraná basin, Argentina. *Zootaxa*, *3391*, 39–51.

Cattel, R. B. (1966). The scree test for the number of factors. *Multivariate Behavioral Research*, *1*, 245–276. https://doi.org/10.1207/s15327906mbr0102_10

Chernoff, B., & Machado-Allison, A. (1990). Characid fishes of the genus *Ceratobranchia*, with descriptions of new species from Venezuela and Peru. *Proceedings of the Academy of Natural Sciences of Philadelphia*, *142*, 261–290.

Deprá, G. C., Graça, W. J., Pavanelli, C. S., Avelino, G. S., & Oliviera, C. (2018). Molecular phylogeny of *Planaltina* Böhlke (Characidae: Stevardiinae) and comments on the definition and geographic distribution of the genus, with description of a new species. *PLoS One*, *13*, e0196291. https://doi.org/10.1371/journal.pone.0196291

Eschmeyer, W. N., Fricke, R., & Van der Laan, R. (2018). *Catalog of fishes: genera, species, references*. Retrieved from http://researcharchive.calacademy.org/research/ichthyology/catalog/fishcatmain.asp

Ferreira, K. A., Menezes, N. A., & Quagio-Grassioto, I. (2011). A new genus and two new species of Stevardiinae (Characiformes: Characidae) with a hypothesis on their relationships based on morphological and histological data. *Neotropical Ichthyology*, *9*, 281–298. https://doi.org/10.1590/S1679-62252011000200005

Fink, W. L., & Weitzman, S. H. (1974). The so-called Cheirodontin fishes of Central America with descriptions of two new species (Pisces: Characidae). *Smithsonian Contributions to Zoology*, *172*, 1–45. https://doi.org/10.5479/si.00810282.172

Frontier, S. (1976). Etude de la dècroissance des valeurs propres dans une analyse en composantes principales: Comparaison avec le modèle du bâton brisé. *Journal of Experimental Marine Biology and Ecology*, *25*, 67–75. https://doi.org/10.1016/0022-0981(76)90076-9

Frota, A., Deprá, G. d. C., Petenucci, L. M., & Graça, W. J. d. (2016). Inventory of the fish fauna from Ivaí River basin, Paraná State, Brazil. *Biota Neotropica*, *16*, e20150151. https://doi.org/10.1590/1676-0611-BN-2015-0151

Hammer, O., Harper, D. A. T., & Ryan P. D. (2001). PAST: Paleontological statistics software package for education and data analysis. *Palaeontologia Electronica*, *4*, 1–9.

Humphries, J. M., Bookstein, F. L., Chernoff, B., Smith, G. R., Elder, R. L., & Poss, S. G. (1981). Multivariate discrimination by shape in relation to size. *Systematic Biology*, *30*, 291–308. https://doi.org/10.1093/sysbio/30.3.291

Mahnert, V., & Géry, J. (1987). Deux nouvelles espèces du genre *Hyphessobrycon* (Pisces, Ostariophysi, Characidae) du Paraguay: *H. guarani n. sp. et H. procerus* n. sp. Bonner Zoologische Beiträge, *38*, 307–314.

Mahnert, V., & Géry, J. (1988). Les genres *Piabarchus* Myers et *Creagrutus* Günther du Paraguay, avec la description de deux espèces nouvelles (Pisces, Ostariophysi, Characidae). *Revue Française d'Aquariologie Herpétologie*, *15*, 1–8.

Malabarba, L. R., & Weitzman, S. H. (2003). Description of new genus with six new species from southern Brazil, Uruguay and Argentina, with a discussion of a putative characid clade (Teleostei: Characiformes: Characidae). *Comunicações do Museu de Ciências e Tecnologia da PUCRS, Série Zoologia*, *16*, 67–151.

Menezes, N. A., & Weitzman, S. H. (1990). Two new species of *Mimagoniates* (Teleostei: Characidae: Glandulocaudinae), their phylogeny and biogeography and a key to the glandulocaudin fishes of Brazil and Paraguay. *Proceedings of the Biological Society of Washington*, *103*, 380–426.

Menezes, N. A., & Weitzman, S. H. (2009). Systematics of the neotropical fish subfamily Glandulocaudinae (Teleostei: Characiformes: Characidae). *Neotropical Ichthyology*, *7*, 295–370. https://doi.org/10.1590/S1679-62252009000300002

Menezes, N. A., & Weitzman, S. H. (2011). A systematic review of *Diapoma* (Teleostei: Characiformes: Characidae: Stevardiinae: Diapomini) with descriptions of two new species from southern Brazil. *Papéis Avulsos de Zoologia*, *51*, 59–82. https://doi.org/10.1590/S0031-10492011000500001

Menezes, N. A., Weitzman, S. H., & Burns, J. R. (2003). A systematic review of *Planaltina* (Teleostei: Characiformes: Characidae: Glandulocaudinae: Diapomini) with a description of two new species from the upper rio Paraná, Brazil. *Proceedings of the Biological Society of Washington*, *116*, 557–600.

Mirande, J. M. (2010). Phylogeny of the family Characidae (Teleostei: Characiformes): From characters to taxonomy. *Neotropical Ichthyology*, *8*, 385–568. https://doi.org/10.1590/S1679-62252010000300001

Mirande, J. M. (2018). Morphology, molecules and the phylogeny of Characidae (Teleostei, Characiformes). *Cladistics*. https://doi.org/10.1111/cla.12345

Mirande, J. M., Jerep, J., & Vanegas-Ríos, J. A. (2013). Phylogenetic relationships of the enigmatic *Carlastyanax aurocaudatus* (Eigenmann) with remarks on the phylogeny of the Stevardiinae (Teleostei: Characidae). *Neotropical Ichthyology*, *11*, 747–766. https://doi.org/10.1590/S1679-62252013000400003

Netto-Ferreira, A. L., Birindelli, J. L. O., Souza, L. M., & Menezes, N. A. (2014). A new species of *Rhinopetitia* Géry 1964 (Ostariophysi: Characiformes: Characidae) from the Rio Teles Pires, Rio Tapajós basin, Brazil. *Journal of Fish Biology*, *84*, 1539–1550. https://doi.org/10.1111/jfb.12384

Protogino, L. C., & Miquelarena, A. M. (2012). *Cyanocharax alburnus* (Hensel, 1870) (Characiformes: Characidae): First distribution record in Argentina. *Check List*, *8*, 581–583. https://doi.org/10.15560/8.3.581

Rohlf, F. J. (2015). The tps series of software. *Hystrix*, *26*, 1–4. https://doi.org/10.4404/hystrix-26.1-11264

Rohlf, F. J., & Bookstein, F. L. (1987). A comment on shearing as a method for "size correction". *Systematic Biology*, *36*, 356–367. https://doi.org/10.2307/2413400

Sabaj, M. H., (2016). *Standard symbolic codes for institutional resource collections in herpetology and ichthyology: An online reference*. Version 6.5 (August 16, 2016). Retrieved from http://www.asih.org/

Taylor, W. R., & Dyke, G. C. V. (1985). Revised procedures for staining and clearing small fishes and other vertebrates for bone and cartilage study. *Cybium*, *9*, 107–119.

Thomaz, A. T., Arcila, D., Ortí, G., & Malabarba, L. R. (2015). Molecular phylogeny of the subfamily Stevardiinae Gill, 1858 (Characiformes: Characidae): Classification and the evolution of reproductive traits. *BMC Evolutionary Biology*, *15*, 146. https://doi.org/10.1186/s12862-015-0403-4

Vanegas-Ríos, J. A. (2017). Phylogeny of the Neotropical genus *Gephyrocharax* (Characiformes: Characidae: Stevardiinae), with remarks on the tribe Stevardiini. *Zoologial Journal of the Linnean Society*, *182*, 808–829. https://doi.org/10.1093/zoolinnean/zlx045 (online).

Vanegas-Ríos, J. A., Azpelicueta, M. M., Mirande, J. M., & Gonzales, M. D. G. (2013). *Gephyrocharax torresi* (Characiformes: Characidae: Stevardiinae), a new species from the Río Cascajales basin, Río Magdalena system, Colombia. *Neotropical Ichthyology*, *11*, 275–284. https://doi.org/10.1590/S1679-62252013000200005

Vari, R. P., & Ortega, H. (2000). *Attonitus*, a new genus of sexually dimorphic characiforms (Ostariophysi: Characidae) from western Amazonia; a phylogenetic definition and description of three new species. *Icthyological Exploration of Freshwaters*, *11*, 113–140.

Weitzman, S. H. (2003). Subfamily Glandulocaudinae. In R. E. Reis, S. O. Kullander, & C. J. Ferraris, Jr. (Eds.), *Check list of the freshwater fishes of South and Central America* (pp. 222–230). Porto Alegre, Brazil: EDIPUCRS.

Weitzman, S. H., & Fink, S. V. (1985). Xenurobryconin phylogeny and putative pheromone pumps in Glandulocaudine fishes (Teleostei: Characidae). *Smithsonian Contributions to Zoology*, *421*, 1–121.

Weitzman, S. H., & Menezes, N. A. (1998). Relationships of the tribes and genera of Glandulocaudinae (Ostariophysi: Characiformes: Characidae) with a description of a new genus, *Chrysobrycon*. In L. R. Malabarba, R. E. Reis, R. P. Vari, Z. M. S. d. Lucena, & C. A. Lucena (Eds.), *Phylogeny and classification of neotropical fishes* (pp. 171–192). Porto Alegre, Brazil: EDIPUCRS.

Weitzman, S. H., Menezes, N. A., Evers, H.-G., & Burns, J. R. (2005). Putative relationships among inseminating and externally fertilizing characids, with a description of a new genus and species of Brazilian inseminating fish bearing an anal-fin gland in males (Characiformes: Characidae). *Neotropical Ichthyology*, *3*, 329–360. https://doi.org/10.1590/S1679-62252005000300002

Zarucki, M., González-Bergonzoni, I., Teixeira-de-Mello, F., Duarte, A., Serra, S., Quintans, F., & Loureiro, M. (2010). New records of freshwater fish for Uruguay. *Check List*, *6*, 4. https://doi.org/10.15560/6.2.191

How to cite this article: Vanegas-Ríos JA, Azpelicueta María de las M., Malabarba LR. A new species of *Diapoma* (Characiformes, Characidae, Stevardiinae) from the Rio Paraná basin, with an identification key to the species of the genus. *J Fish Biol*. 2018;93:830–841. https://doi.org/10.1111/jfb.13786